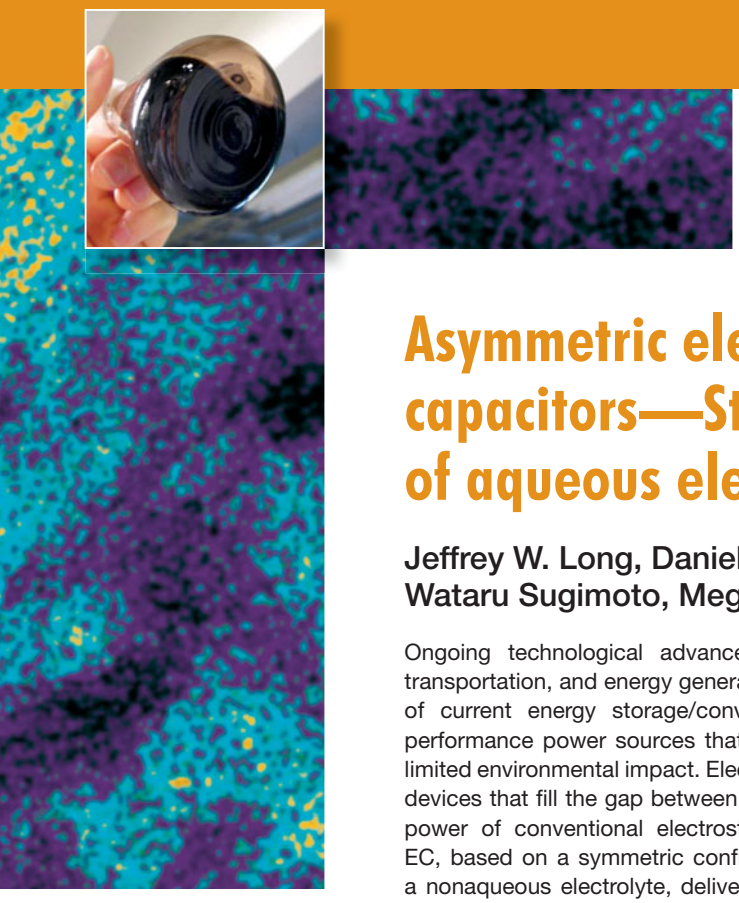

Asymmetric electrochemical capacitors—Stretching the limits of aqueous electrolytes

Jeffrey W. Long, Daniel Bélanger, Thierry Brousse, Wataru Sugimoto, Megan B. Sassin, and Olivier Crosnier

Ongoing technological advances in such disparate areas as consumer electronics, transportation, and energy generation and distribution are often hindered by the capabilities of current energy storage/conversion systems, thereby driving the search for high-performance power sources that are also economically viable, safe to operate, and have limited environmental impact. Electrochemical capacitors (ECs) are a class of energy-storage devices that fill the gap between the high specific energy of batteries and the high specific power of conventional electrostatic capacitors. The most widely available commercial EC, based on a symmetric configuration of two high-surface-area carbon electrodes and a nonaqueous electrolyte, delivers specific energies of up to ~6 Whkg^{-1} with sub-second response times. Specific energy can be enhanced by moving to asymmetric configurations and selecting electrode materials (e.g., transition metal oxides) that store charge via rapid and reversible faradaic reactions. Asymmetric EC designs also circumvent the main limitation of aqueous electrolytes by extending their operating voltage window beyond the thermodynamic 1.2 V limit to operating voltages approaching ~2 V, resulting in high-performance ECs that will satisfy the challenging power and energy demands of emerging technologies and in a more economically and environmentally friendly form than conventional symmetric ECs and batteries.

Electrochemical capacitors as an energy-storage solution

Electrochemical capacitors (ECs, also commonly denoted as "supercapacitors" or "ultracapacitors") represent an emerging class of energy-storage devices whose particular performance characteristics fill the gap on the energy versus power spectrum between the high specific power provided by conventional capacitors and the high specific energy provided by batteries (see **Figure 1**).[1–4] Electrochemical capacitors are distinguished from their solid-state electrostatic capacitor counterparts by storing charge at electrochemical interfaces, where the effective capacitances are orders of magnitude greater than those obtained by storing charge in an electric field imposed across a conventional dielectric. The enhanced specific energy of ECs comes with some tradeoff in specific power because of the fundamental requirements to transport ions and solvent during charge–discharge operation.

In terms of both design and function, batteries and ECs are closely related, being based on electrochemical cells comprising two opposing electrodes separated by a liquid or solid electrolyte containing mobile ions. Batteries are typically designed to provide maximum energy by storing charge in bulk electrodes through faradaic reactions, while ECs rely on near-surface charge-storage mechanisms (e.g., double-layer capacitance or redox pseudocapacitance) to achieve greater specific power at some expense of specific energy. While present ECs are limited in specific energy (3–6 W h kg^{-1} versus >100 W h kg^{-1} for an advanced Li-ion battery), they provide the ability to store and release that energy over timescales of a few seconds and exhibit extended cycle life (hundreds of thousands of cycles) that no battery can achieve.

Jeffrey W. Long, U.S. Naval Research Laboratory, Washington, DC 20375, USA; jeffrey.long@nrl.navy.mil
Daniel Bélanger, Département de Chimie, Université du Québec à Montréal, Canada H3C 3P8; belanger.daniel@uqam.ca
Thierry Brousse, University of Nantes, France; thierry.brousse@univ-nantes.fr
Wataru Sugimoto, Shinshu University, Ueda, Nagano 386-8567, Japan; wsugi@shinshu-u.ac.jp
Megan B. Sassin, U.S. Naval Research Laboratory, Washington, DC 20375, USA; megan.sassin@nrl.navy.mil
Olivier Crosnier, University of Nantes, France; olivier.crosnier@univ-nantes.fr
DOI: 10.1557/mrs.2011.137

Report Documentation Page

Form Approved
OMB No. 0704-0188

1. REPORT DATE	2. REPORT TYPE	3. DATES COVERED
JUL 2011		**00-00-2011 to 00-00-2011**

4. TITLE AND SUBTITLE	5a. CONTRACT NUMBER
Asymmetric electrochemical capacitors-Stretching the limits of aqueous electrolytes	5b. GRANT NUMBER
	5c. PROGRAM ELEMENT NUMBER
6. AUTHOR(S)	5d. PROJECT NUMBER
	5e. TASK NUMBER
	5f. WORK UNIT NUMBER
7. PERFORMING ORGANIZATION NAME(S) AND ADDRESS(ES) **U.S. Naval Research Laboratory,Washington,DC,20375**	8. PERFORMING ORGANIZATION REPORT NUMBER
9. SPONSORING/MONITORING AGENCY NAME(S) AND ADDRESS(ES)	10. SPONSOR/MONITOR'S ACRONYM(S)
	11. SPONSOR/MONITOR'S REPORT NUMBER(S)

12. DISTRIBUTION/AVAILABILITY STATEMENT
Approved for public release; distribution unlimited

13. SUPPLEMENTARY NOTES
MRS BULLETIN,VOLUME 36, JULY 2011

14. ABSTRACT

15. SUBJECT TERMS

16. SECURITY CLASSIFICATION OF:			17. LIMITATION OF ABSTRACT	18. NUMBER OF PAGES	19a. NAME OF RESPONSIBLE PERSON
a. REPORT **unclassified**	b. ABSTRACT **unclassified**	c. THIS PAGE **unclassified**	**Same as Report (SAR)**	**11**	

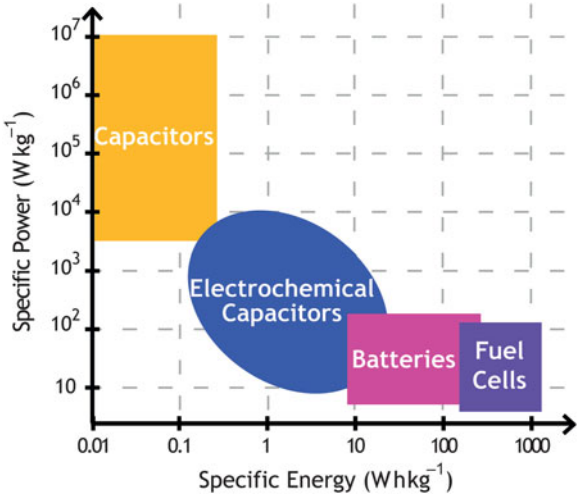

Figure 1. Specific power versus specific energy plot comparing common electrical energy-storage devices.

With nonstop advances in new power-hungry technologies, ECs are attracting attention as energy-storage solutions. The fast symmetric charge–discharge characteristics and long cycle life of ECs are particularly well suited to capture and reuse energy from repetitive motion (automotive braking, elevator operation, lift/release of cargo cranes) that would otherwise be wasted, resulting in improved energy efficiency and reduced environmental emissions.[5] When combined in a hybrid power system with energy-dense, but power-limited components (conventional battery, fuel cell, combustion engine), ECs can enhance lifetime, reduce total system weight and volume, and increase the efficiency by bearing the burden of periodic pulse-power demands that would otherwise compromise the energy-dense component.[5,6] Electrochemical capacitors are also being deployed in the utilities sector for backup/bridge power and load-leveling to provide higher quality power (with fewer sags and spikes) and reduce economic losses that result from power disruptions.

Electric double-layer capacitors

The simplest and most commercially advanced EC is the electric double-layer capacitor (EDLC), invented by the Standard Oil Company of Ohio in 1966,[7] whose basic design includes a symmetric cell configuration* comprising two high-surface-area carbon electrodes separated by a nonaqueous electrolyte. As the name implies, charge is stored in the electric double-layer that arises at all electrode/electrolyte interfaces (see **Figure 2**a), resulting in effective capacitances of 10–40 μF cm^{-2}. The specific energy of the EDLC (E_{cell}) depends on both the cell-level specific capacitance (C, a series combination of the capacitances of the individual electrodes) and operating voltage (V_{cell}) via the relationship,[1]

$$E_{cell} = \tfrac{1}{2} C V_{cell}^2. \quad (1)$$

The specific capacitance is maximized by choosing high surface area, lightweight electrode materials, such as activated carbon, while nonaqueous electrolytes are often chosen to maximize the operating voltage, which is primarily determined by the stable potential window of the electrolyte (e.g., ~2.7 V for EDLCs with acetonitrile-based electrolytes), as opposed to aqueous-based electrolytes that exhibit a more limited potential window. EDLCs are now widely available from many international manufacturers/suppliers[8–10] in forms ranging from small single-cell 2.7 V capacitors of a few farads to integrated modules of EDLCs that operate at voltages relevant for large-scale applications (e.g., 125 V).

While EDLCs are steadily gaining acceptance in the commercial marketplace as a proven energy-storage solution, research continues at the fundamental and applied levels, particularly with regard to developing and adapting new electrode and electrolyte materials. For example, many forms of nanostructured carbons,[11–14] including aerogels,[15] nanotubes,[16] carbide-derived carbons,[17] and graphene,[18,19] are being explored as alternatives to activated carbon, with the goal of improving

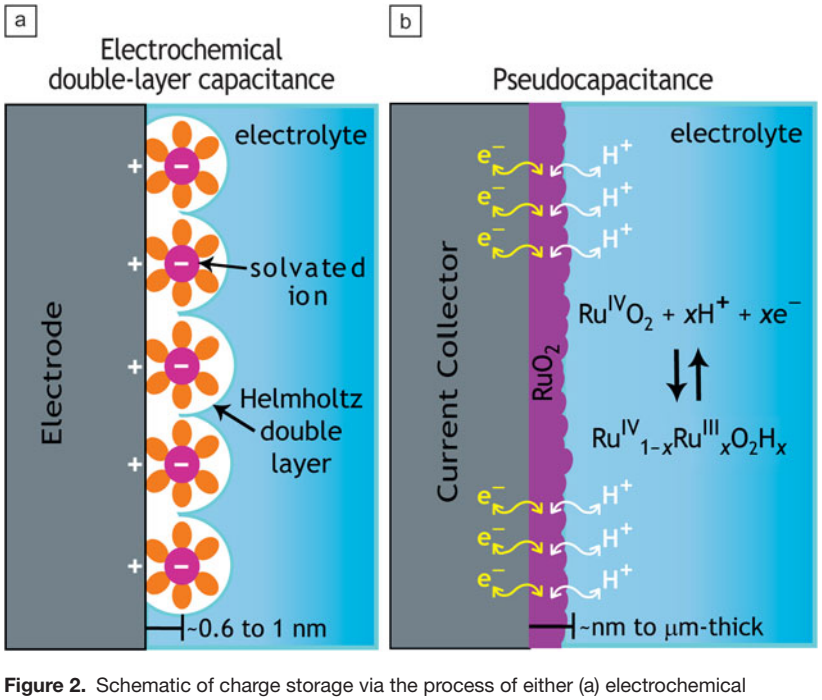

Figure 2. Schematic of charge storage via the process of either (a) electrochemical double-layer capacitance or (b) pseudocapacitance.

*The symmetric EC design uses two electrodes with the same active materials in the positive and negative electrodes. The asymmetric EC design is related in the present article to the use of two electrodes made of different materials, in which the charge-storage mechanism can be either capacitive, pseudocapacitive, or faradaic.

specific energy while maintaining high specific power in the ultimate EDLC. Advanced electrolytes are also being investigated to extend the operating voltages of EDLCs with corresponding improvements in specific energy.[20] Despite these advancements, the ultimate specific energies of EDLCs are fundamentally limited by their reliance on double-layer capacitance as the primary charge-storage mechanism, because in this case, the device capacity Q (C g^{-1} or C L^{-1}) is directly proportional to the device capacitance C (F g^{-1} or F L^{-1}) according to $Q = C\,V_{cell}$.

Amplifying charge-storage in ECs via redox-based pseudocapacitance

The limitations of storing charge only as double-layer capacitance can be circumvented by selecting active materials that undergo rapid and reversible electron-exchange reactions at or near the electrode surface (see Figure 2b). Such materials often express broad and symmetric charge–discharge profiles that are reminiscent of those generated by double-layer capacitance, thus the term "pseudocapacitance" is used to describe their charge-storage mechanism.[21–23] Ruthenium oxide is perhaps the best-known material that exhibits pseudocapacitance, but many other transition metal oxides, metal nitrides,[24,25] and conducting polymers[26] demonstrate similar electrochemical responses. Pseudocapacitance-based charge storage is most effective in aqueous electrolytes, and the corresponding enhancements in charge-storage capacity can compensate for the restricted voltage window of water, resulting in energy densities for aqueous ECs that are competitive with nonaqueous EDLCs with the additional advantage of using a nonflammable electrolyte (water-based).

Ruthenium oxides as the "gold standard" for pseudocapacitance

Various forms of ruthenium oxide, ranging from nanocrystalline rutile RuO_2 to disordered hydrous $RuO_2{\bullet}xH_2O$, exhibit pseudocapacitance when electrochemically cycled in acidic aqueous electrolytes. The pseudocapacitive behavior of RuO_2 is generally ascribed to a series of fast, reversible electron-transfer reactions that are coupled with adsorption of protons at or near the electrode surface (see Figure 2b).[1]

$$Ru^{IV}O_2 + xH^+ + xe^- \leftrightarrow Ru^{IV}_{1-x}Ru^{III}_{x}O_2H_x \qquad (2)$$

The performance of ruthenium oxides for pseudocapacitive charge-storage ranges from tens to hundreds of farads per gram, determined by factors such as the degree of crystallinity, particle size, and electrode architecture. For example, Zheng et al. investigated sol–gel-derived hydrous RuO_2 as a function of heat treatment and obtained the highest specific capacitance (720 Fg^{-1}) for RuO_2 forms of intermediate crystallinity and degrees of hydration (e.g., $RuO_2{\bullet}0.5H_2O$).[27] Subsequent structural[28,29] and electrochemical[28–30] investigations of a related series of hydrous ruthenium oxides demonstrated that the maximum specific capacitance is achieved when solid-state electron and proton transport is balanced, facilitated by a nanocomposite RuO_2 structure comprising interpenetrating networks of nanocrystalline rutile RuO_2 and hydrous, disordered phases (see **Figure 3**).[28] A related example of the interplay of electron and proton conduction is found in two-dimensional RuO_2 nanosheets (see **Figure 4**), which show the clearest evidence for faradaic charge storage (in the form of well-defined redox peaks) while approximating the performance of hydrous RuO_2.[31–33] The charge-storage properties of ruthenium oxides can be further enhanced by dispersing them on high-surface-area carbon substrates, where RuO_2-normalized values of up to 1200 F g^{-1} have been reported,[34–36] or when expressed as nanometers-thick coatings on porous silica filter paper.[37]

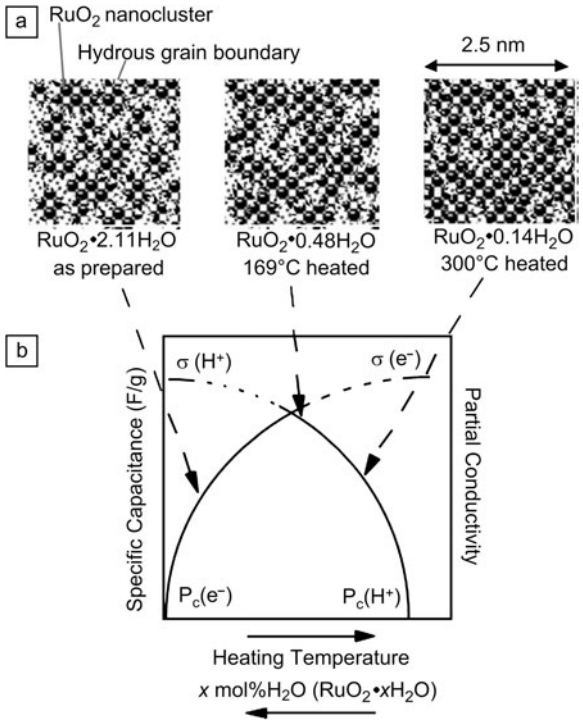

Figure 3. Illustrations of the variation in the solid-state structure of RuO_2 as a function of water content (a) and a plot showing the interplay of electronic, σ (e^-), and protonic conductivity, σ (H^+), with specific capacitance for the same RuO_2 series (b). Reprinted with permission from Reference 27. ©2002, American Chemical Society.

In addition to the high gravimetric capacitance, the volumetric capacitance is another attractive rationale for using RuO_2, as its density is much higher than most conventional carbon-based materials. Despite these performance advantages, the high cost of RuO_2-based ECs limits their application to small-scale, high-value-added devices where miniature-sized, flexible, or translucent characteristics are desired.[38,39]

Manganese oxide as a low-cost alternative

The high costs of oxides based on ruthenium (a platinum-group metal) have prompted the search for less-expensive metal oxides that also display pseudocapacitance, with manganese oxides (MnOx) as the prime example. Lee and Goodenough were the first to report capacitance-like behavior for

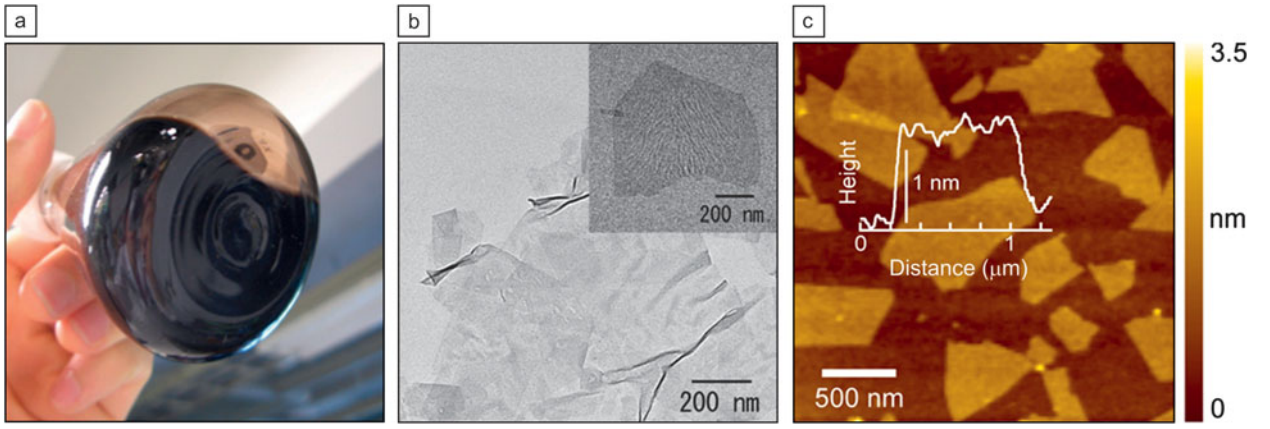

Figure 4. (a) Photograph of a colloidal sol of RuO_2 nanosheets; (b) transmission electron micrograph; and (c) atomic force micrograph of RuO_2 nanosheets.

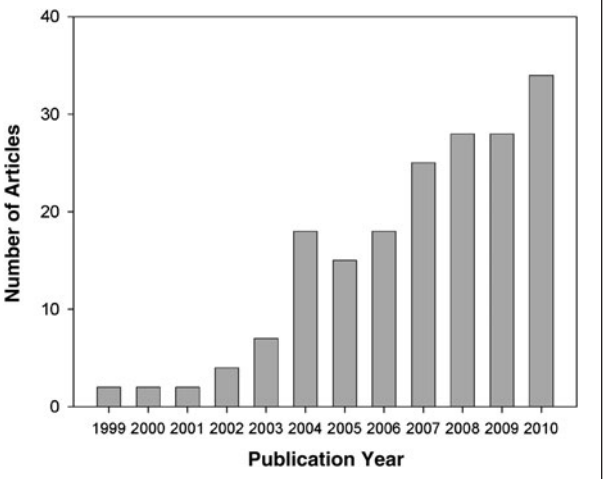

Figure 5. Charting the number of peer-reviewed publications on the use of manganese oxides for electrochemical capacitor applications as a function of the year published. (Results collected using the ISI *Web of Science* database and "manganese" and "capacitor" as search terms.)

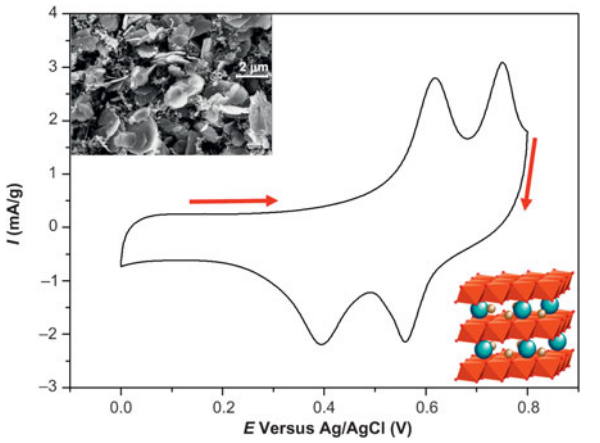

Figure 6. Scanning electron micrograph of a birnessite-type MnO_2–carbon black composite electrode and corresponding cyclic voltammogram (where *E* refers to the electrode potential, and *I* to the measured current) in 0.5 M Na_2SO_4 at 2 mV s^{-1}. Schematic of the birnessite-type MnO_2 structure with MnO_6 octahedra layers (red) separated by water molecules (blue) and K^+ or Na^+ cations (gold).

manganese oxide when electrochemically cycled in mild aqueous electrolytes† (e.g., 2 M KCl),[40] and their initial findings have since catalyzed interest in manganese oxides as active materials for electrochemical capacitor applications (see **Figure 5**).[41–43] The extensive body of literature on MnOx-based materials for ECs now covers many synthetic methods, MnOx polymorphs (amorphous to highly crystalline; see **Figure 6**), and electrode structures (thin films, powder composites, advanced three-dimensional architectures), resulting in a wide range of electrochemical performance metrics.

The continued evolution of MnOx-based electrode materials for EC applications requires a more thorough understanding of the pseudocapacitance mechanism and of the interplay between electrode structure and electrochemical performance. Spectroscopic techniques such as x-ray photoelectron spectroscopy[44] and x-ray absorption spectroscopy[45] confirm that the average Mn oxidation state toggles in varying degrees between +3 and +4, compensated by the reversible insertion of cations (e.g., Na^+, K^+) and/or protons from the contacting mild aqueous electrolyte (see schematic in Figure 6).[45,46]

$$MnO_2 + X^+ + e^- \leftrightarrow MnOOX, \quad \text{where } X^+ = H^+, Li^+, Na^+, \text{or } K^+. \tag{3}$$

The existence of over 20 polymorphs of manganese oxide further complicates the interpretation of the pseudocapacitance mechanism, which may vary as a function of crystal structure (or lack thereof), water content, and the presence of intercalated cations.[44,47]

†"Mild" refers to a near-neutral ($5 \le pH \le 9$) aqueous-based solution.

More general insight can be gained by comparing thin-film and powder-composite MnOx electrodes. Thin-films of the oxide (tens to hundreds of nanometers thick) deposited at planar electrodes[48] often yield specific capacitances that reach >50% of the theoretical value (1233 F g^{-1} for a full one-electron redox reaction: $Mn^{4+/3+}$),[49] whereas powder composites typically yield 10–20% of the theoretical limit,[40,50] suggesting that only a thin volume of the MnOx electrode participates in the charge-storage reaction under electrochemical capacitor demands. Although the high specific capacitances of nanometric MnOx films (now competitive with RuO_2) are alluring, ECs incorporating such ultrathin films in planar 2D forms would not provide technologically relevant charge-storage capacity when normalized to the device footprint. The benefits of the high redox utilization and facile kinetics observed with nanoscale MnOx films can be translated into 3D electrode architectures in which MnOx coatings are applied to ultraporous, conductive substrates (see **Figure 7**). Various nanostructured carbons, including templated mesoporous carbon,[51] nanotubes,[52–55] nanofoams,[56] and graphene[57] have been used as base structures for MnOx-modified electrode architectures that show enhanced performance relative to conventional powder-composite carbon−MnOx electrodes.

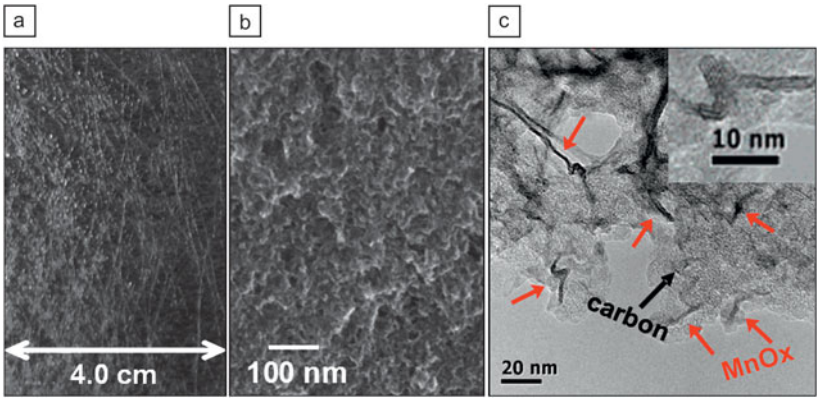

Figure 7. A MnOx-coated carbon nanofoam as imaged by (a) optical microscopy, (b) scanning electron microscopy, and (c) transmission electron microscopy at low and high magnification (inset). Adapted and reprinted with permission from Reference 56. ©2007, American Chemical Society.

In terms of specific capacitance, MnOx-based materials demonstrate a clear advantage compared to carbon-based materials that rely on double-layer capacitance. However, the operating voltage window of MnOx in the mild aqueous electrolytes described previously is limited by the oxygen evolution reaction on the positive end and by the irreversible reduction of Mn^{4+} to Mn^{3+} and subsequent disproportionation to soluble Mn^{2+} on the negative side.[58,59] These two processes restrict the operating cell voltage of a symmetric MnOx//MnOx EC to ≤0.9V (see **Figure 8**a),[60,61] negating some of the positive effects of the MnOx pseudocapacitance enhancements, and resulting in cell-level energy densities that are not competitive with state-of-the-art EDLCs.

Asymmetric‡ electrochemical capacitors with aqueous electrolytes: The best of both worlds

The development of electrode materials that exhibit faradaic pseudocapacitance with high-rate charge–discharge characteristics now enables a new class of ECs in which two distinct electrodes are paired in an asymmetric configuration: (1) a "pseudocapacitive" (e.g., MnO_2, see Figure 8b) or "battery-type" (e.g., PbO_2, see Figure 8c) positive electrode that relies on faradaic mechanisms for charge storage versus (2) a high-surface-area carbon negative electrode (see Figure 8b and 8c), where charge is stored primarily as double-layer capacitance.[62,63] The asymmetric design blends the best performance characteristics of ECs and batteries, increasing the capacity of the device via the faradaic charge-storage mechanisms of the positive electrode, while maintaining fast charge–discharge response due to the double-layer capacitance mechanism at the negative electrode. Further, when used in an asymmetric configuration, the high overpotentials for H_2 and O_2 evolution at the carbon-based negative electrode and pseudocapacitive or battery-like positive electrode, respectively, extend the effective voltage window of aqueous electrolytes beyond the thermodynamic limit (~1.2 V), resulting in significantly higher specific energy than for symmetric ECs with aqueous electrolytes (see Figure 8b and 8c). The use of aqueous electrolytes supports high-power operation because of their high ionic conductivity and high concentrations of ions, while providing cost and safety advantages of a water-based electrolyte compared to energy-storage technologies that incorporate nonaqueous electrolytes (e.g., EDLCs and Li-ion batteries). The use of an aqueous electrolyte with simple salts (ACl, A_2SO_4, ANO_3, A=Li, Na, K) minimizes the need for extensive purification and handling under a controlled atmosphere (no need for a dry room or glove box), simplifying the fabrication and packaging process. The use of a faradaic material with a fixed thermodynamic potential may lessen self-discharge in asymmetric ECs, while the large capacity of the faradaic material also ensures that the full double-layer capacitance of the negative electrode is utilized during cell operation.[62]

Early examples of this "asymmetric aqueous EC" design were based on an activated carbon negative electrode paired

‡The asymmetric EC design and its name was first described in U.S. Patent 6,222,723, where the device has different electrode materials and the capacitance ratio of the two electrodes is >3, preferably >10. Although the carbon//MnO_2 EC does not exactly match this definition (different electrode materials but similar capacitance for both electrodes), it is also denoted as "asymmetric" because of similarities in design.

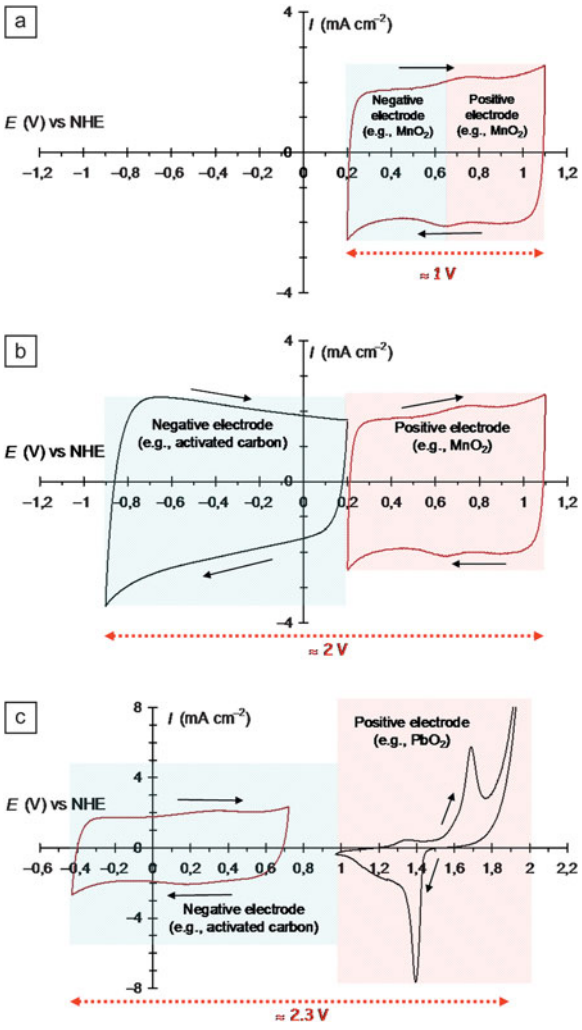

Figure 8. Schematic representation of cyclic voltammograms for three different configurations of aqueous-based electrochemical capacitors (ECs) in which areas shaded in red and blue represent the potential window of the positive and negative electrode, respectively for: (a) symmetric MnO_2//MnO_2 EC with α-MnO_2 electrodes in 0.5 M K_2SO_4; (b) asymmetric activated carbon//MnO_2 EC in 0.5 M K_2SO_4; and (c) asymmetric activated carbon//PbO_2 EC in 1 M H_2SO_4. NHE, normal hydrogen electrode; *I*, measured current; and *E*, electrode potential.

with either a PbO_2 or an NiOOH faradaic positive electrode in an acidic or alkaline electrolyte, respectively.

$$PbO_2 + 4H^+ + SO_4^{2-} + 2e^- \leftrightarrow PbSO_4 + 2H_2O \quad (4)$$

$$NiOOH + H_2O + 1e^- \leftrightarrow Ni(OH)_2 + OH^- \quad (5)$$

Commercialized variants of both the carbon//NiOOH[64] and carbon//PbO_2[65] asymmetric EC designs are already deployed for niche applications that require particular combinations of specific energy and power. Typical specific energies for these packaged devices range from ~8–10 W h kg^{-1} for carbon//NiOOH to 25 W h kg^{-1} for carbon//PbO_2, compared to the 3–6 W h kg^{-1} of symmetric EDLCs. The PbO_2- and NiOOH-based asymmetric ECs are fabricated with internal electrode architectures that are more characteristic of conventional batteries, resulting in bulkier individual electrodes than those used in EDLCs, which degrades charge–discharge times to the order of a few minutes rather than the few-second response characteristic of EDLCs.

The cost and toxicity of lead and nickel oxides and their associated extreme-pH electrolytes (highly acidic and basic, respectively) make carbon//MnOx asymmetric ECs with mild pH electrolytes an attractive alternative in terms of safety and manufacturability. Manganese oxide-based ECs are still a relatively immature technology, but lab-scale prototypes demonstrate promising specific energies ranging from 10–28 W h kg^{-1}.[66–68] Further advances in performance at the materials level should continue to drive the development and commercialization of carbon//MnOx asymmetric ECs as an attractive energy-storage technology for applications where a combination of both moderate specific energy and fast response times are required (e.g., for energy capture in regenerative-braking processes). For example, a MnO_2 electrode combined with a negative activated carbon electrode leads to an extended cell voltage (2 V versus 0.9 V for the symmetric design, see Figure 8a and 8b)[41] and a fivefold increase in maximum specific energy.

The negative electrode: Activated carbon and beyond

The specific energies of aqueous asymmetric ECs are further enhanced by adventitious pseudocapacitance mechanisms at the surfaces of carbon-based negative electrodes when scanned to progressively more negative potentials in aqueous electrolytes.[69–71] This anomalous pseudocapacitance behavior is typically ascribed to an "electrochemical hydrogen storage" process in which H_2O from the electrolyte is initially reduced at the electrode, followed by adsorption of atomic hydrogen at the carbon surface (see Equations 6 and 7).[72–74]

$$H_2O + e^- \rightarrow H + OH^- \quad (6)$$

$$C + H \rightarrow CH_{ad} \quad (7)$$

Adsorbed hydrogen atoms (H_{ad}) are released from the carbon surface and recombine with OH^- as the electrode is discharged, although typically with considerable hysteresis between the charge and discharge potentials. The pseudocapacitance enhancements at carbon negative electrodes depend on a number of factors, including pore structure, surface functionality,[75] and the inclusion of metals such as Ni that catalyze the hydrogen adsorption/desorption mechanism.[70] Pseudocapacitive functionalities can also be deliberately introduced on carbon surfaces to improve charge-storage capacity (see **Figure 9**), as was recently shown for anthraquinone-modified carbon.[76,77]

High-surface-area carbons provide attractive specific capacitances (150–250 F g^{-1}) when used in either strongly acidic or alkaline aqueous electrolytes, but their performance is more limited in moderate-pH electrolytes, where

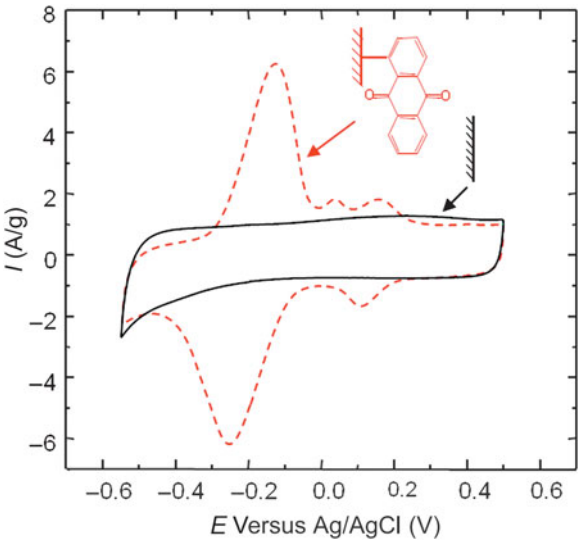

Figure 9. Cyclic voltammograms in 0.1 M H_2SO_4 at a scan rate of 10 mVs^{-1} for unmodified activated carbon electrode (—) and activated carbon chemically modified with 11 wt% (- - -) anthraquinone covalently grafted to carbon via a diazonium-based precursor. Adapted and reprinted with permission from Reference 77. *I*, measured current; *E*, electrode potential.

specific capacitances of 100–120 F g^{-1} are typical.[78] The growing interest in MnOx-based ECs, which use such mild aqueous electrolytes, has also spurred interest in alternative negative electrode materials that exhibit pseudocapacitance in a complementary potential window to that for MnOx. Iron oxides were among the first such materials investigated,[79–82] while other metal oxides such as SnO_2[82] and TiO_2,[84,85] metal phosphates ($Li(Ti_2(PO_4)_3)$,[86] and conducting polymers (e.g., polyaniline, polypyrrole)[68] are also potential contenders as negative electrodes for MnOx-based ECs.

Design and evaluation of asymmetric ECs at the electrode and device level

The electrochemical data reported in the literature for aqueous asymmetric ECs vary widely (see **Figure 10**). Nominally similar materials or device configurations may exhibit significantly different values of capacitance that arise because of variations in electrode fabrication, active material loading, or electrochemical testing procedures.[41,42,87–89] Confusion may also arise when the results of single-electrode measurements in a three-electrode configuration are inappropriately extrapolated to predict device-level performance metrics (e.g., in a symmetric device, the device-level specific capacitance is, at best, only 25% of the single-electrode capacitance).[3] While single-electrode measurements are valuable for determining the capacitance, stable potential window, and cycling stability of new active materials, such measurements should not be used to calculate specific energy or specific power, which requires the fabrication and testing of a two-electrode device.

Although the construction of an EC is seemingly simple (two electrodes, a separator, and electrolyte), several subtle design parameters must be considered in order to optimize the electrochemical performance (e.g., electrode composition and thickness, active material loading, pressure applied to the stack). The most difficult challenge is to balance the accessible charge-storage capacities of the opposing electrodes that comprise the EC. In the case of symmetric ECs, where each electrode has the same nominal specific capacitance, achieving cell balance may still be difficult if the rest potential of the electrodes is not centered within the potential window of the electrolyte (see Figure 8a). Moving from the symmetric to asymmetric EC design provides new opportunities for increasing cell voltage and corresponding energy density (see Figure 8b and 8c), but further complicates cell-balance requirements.

When designing an asymmetric EC that uses capacitive and/or pseudocapacitive electrodes such as a carbon//MnO_2 device, one should first characterize the individual positive and negative electrodes to determine their respective capacities and stable potential windows.[90,91] With this information, the masses of the two electrodes can be adjusted to achieve optimal cell balance in the ultimate EC, thereby not only promoting maximum cell-level capacitance and voltage, but also ensuring that the individual electrodes remain in their respective potential windows for stable operation and improved cycle life.

Electrochemical capacitors with a "battery-type" positive electrode (e.g., PbO_2 or NiOOH) can achieve even higher capacitance values with respect to their pseudocapacitive counterparts (MnOx). In reality, such asymmetric ECs using a purely faradaic electrode require an excess of the

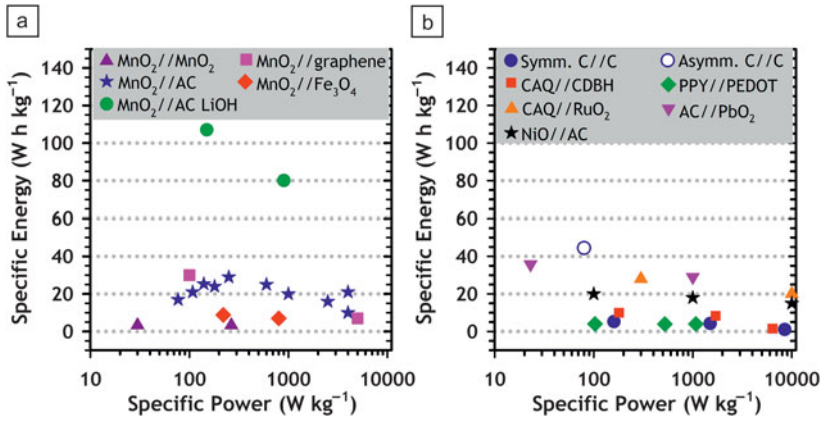

Figure 10. Ragone plots for (a) MnO_2-based aqueous electrochemical capacitors (ECs) and (b) alternative (i.e., non-MnO_2) aqueous-based ECs. AC, activated carbon; CAQ, anthraquinone on carbon; CDBH, dihydroxybenzene on carbon; PPY, polypyrrole; PEDOT, Poly-(3,4-ethylenedioxythiophene). Data are extracted from literature references. Specific energy (E_{cell}) is calculated from Equation 1 and specific power from $P_{real} = E_{cell}/t_{dis}$ (t_{dis} being the operational discharge time).

battery-type electrode in order to ensure long-term cycling stability, partially offsetting anticipated gains in specific energy.[62] The selected asymmetry ratio is chosen to meet cycle life requirements of the application (e.g., a 3:1 ratio will mean the "battery" electrode will have greater depths of discharge than a 10:1 ratio). When projecting specific energies of new ECs for real-world applications, one must ultimately account for such factors as the mass and volume of current collectors, electrolytes, separators, and packaging,[§] which can reduce the effective specific energy by a factor of 4–5 versus normalizing only to the active electrode mass or volume, a practice commonly observed in the literature, as noted by Burke and Miller[92] and Zheng.[93]

Confusion and uncertainty are rife in the literature concerning the useable power capability of asymmetric ECs. The two approaches most often applied to determine the power capability of devices are (1) matched impedance power and (2) real specific power obtained by dividing specific energy by operational discharge (charge) time. Other methods have been used for commercial devices such as (1) the min/max method of the U.S. Advanced Battery Consortium[94] and (2) the pulse energy efficiency approach used at the University of California, Davis.[92] In the case of an in-lab cell, the determination of specific power may be influenced by the particulars of cell assembly, the pressure applied to the stack, the amount of electrolyte, and the type of separator so that the evaluation of specific power (determined using the equivalent series resistance, R), although normalized,[3,14,92] is often neither representative of a future "commercial" device nor comparable with other literature values.

Literature reports of specific power are also more widely scattered than those for specific energy, primarily due to differences in the loading and thickness of the active electrode material. For standard electrodes in a commercial EC, the average thickness is 200 μm, and the mean porosity reaches 70% volume, which would correspond to an average loading of 12 mg cm^{-2} of activated carbon and 24 mg cm^{-2} of MnO_2 in an asymmetric carbon//MnOx EC. While the reported specific power of many thin-film (nanometers to tens of micrometers) electrodes and devices are impressive, those high-power characteristics may not translate when such materials are used at more technologically relevant electrode loadings.

The most pertinent parameter for comparing asymmetric ECs is the typical resistor–capacitor (RC) time constant ($\tau_0 = RC$; ~1–5 s for standard symmetric EDLC). This time constant corresponds to the transition between resistive behavior at frequencies higher than $1/\tau_0$ and capacitive behavior for frequencies lower than $1/\tau_0$.[95] In the case of symmetric or asymmetric ECs, the time constant describes both the discharge and charge of the device, a distinctive characteristic of ECs that contrasts with high-power batteries, where discharge is fast, but recharging requires more time at lower rates, typically one hour or more.

Figure 10 summarizes specific power and energy for a series of aqueous-electrolyte ECs.[41,60,61,66,67,79,96–112] As shown in Figure 10a, the specific energy values of MnOx-based devices follow the expected trend, with symmetric MnOx//MnOx ECs showing lower specific energy than 2 V-rated asymmetric carbon//MnOx ECs. Further enhancements in specific energy are realized if the mild aqueous electrolyte (e.g., 0.6 M K_2SO_4) is replaced with an alkaline electrolyte (e.g., 1 M LiOH).[99] The performance of the negative electrode is another key factor in determining energy/power characteristics. Although graphene is a popular topic of research and has demonstrated outstanding performance in symmetric EDLC devices,[19] it has yet to show significant advantages as a negative electrode for asymmetric ECs relative to conventional activated carbon or as a conductive additive in MnOx-based positive electrodes.[97] Metal oxide-based negative electrodes (e.g., iron oxides) may provide advantages over carbon in terms of volumetric capacitance and energy density, but with potential tradeoffs in gravimetric energy density.[113,114]

Alternative asymmetric designs have also been proposed and are presented in Figure 10b. Symmetric carbon//carbon devices in H_2SO_4[105] and conducting polymer-based ECs[109] both exhibit low specific energy relative to asymmetric designs that are based on a metal oxide positive electrode and carbon negative electrode. Carbon//PbO_2[108] and carbon//NiOOH[111] ECs reported in the literature are also less promising than expected from the projected performance[41] because their specific energies are in the same range as for asymmetric carbon//MnOx ECs. Another way to enhance specific energy of asymmetric devices consists of modifying the activated carbon surface functionalities either by thermal treatment[86] or by chemical grafting of electroactive molecules that boost the capacitance of the carbon by the addition of a faradaic component.[76]

Future outlook for asymmetric aqueous ECs as an energy-storage technology

Aqueous asymmetric ECs offer many attractive features, including: (1) simplified fabrication and packaging procedures that do not require rigorous environmental controls; (2) a higher degree of safety than organic-based ECs with respect to thermal stability and runaway**;[115] (3) the use of less toxic and lower-cost electrolytes; and (4) specific energy that meets or exceeds those of nonaqueous EDLCs. The advancement of aqueous asymmetric ECs will require further improvements in specific power, which is fundamentally limited by the charge-transfer kinetics associated with pseudocapacitance (e.g., MnOx) or battery-like (e.g., PbO_2 and NiOOH) mechanisms. Continuing

[§]Packaging can be a polymer or metal casing with different shapes (cylindrical, prismatic). Material and design are chosen according to the solvent used for the electrolyte and the expected volume/weight of the final cell.

**Thermal runaway describes the situation where overheating a cell results in a further increase in temperature. This uncontrolled increase in temperature can have dramatic consequences, such as melting or vaporization of cell components and cell rupture.

developments in electrode architectures and nanoscale materials should minimize this limitation.

The use of water-based electrolytes also introduces practical challenges with respect to current collectors, temperature-dependent performance, and long-term cycling stability. Current collectors compatible with aqueous electrolytes (stainless steel, nickel, lead) tend to be heavier and more expensive than the thin (25 μm) aluminum foil current collectors used in nonaqueous EDLCs. The corrosion of these current collectors must also be minimized to ensure long-term cycling performance. The extended voltage window made available by the asymmetric EC design must also be carefully managed to avoid extraneous gas evolution at higher cell voltages, a problem that may be mitigated by the presence of carbon as a catalyst for water recombination or by the addition of alternative catalysts to the system.[116] The low-temperature performance, typically below 0°C down to –30°C, of aqueous-based ECs using an MnOx positive electrode and operated in mild aqueous electrolytes (K_2SO_4, KCl) can be a limitation compared to nonaqueous EDLCs, but the use of highly concentrated electrolytes (5 M $LiNO_3$, carbon//MnOx ECs) partially mitigates this issue.[117] The long-term cycling stability of EDLCs (hundreds of thousands of cycles) is difficult to match due to the more complex pseudocapacitance mechanisms relative to the physical nature of double-layer capacitance. Much work remains to be done in order to demonstrate extended cycle life for asymmetric aqueous ECs, although 200,000 cycles were recently reported for an optimized carbon//MnOx EC.[118]

The commercial viability and technological relevance of electrochemical capacitors is presently being demonstrated with carbon//carbon EDLCs in an ever-expanding range of applications. Aqueous asymmetric ECs are a logical choice as the next-generation EC technology due to their potential for enhanced specific energy, reduced costs, and safer cell chemistries compared to present EDLCs. The continuing maturation of such new EC designs will require ongoing research efforts, with a particular emphasis on the development of new high-performance electrode materials and architectures and a more detailed understanding of underlying electrochemical processes that support high charge-storage capacity and long-term cycling stability. Such advances will enable aqueous asymmetric ECs to further bridge the energy/power performance gap between conventional batteries and EDLCs in a form that offers significant advantages in terms of cost and safety.

Acknowledgments

J. Long and M. Sassin acknowledge the financial support of the U.S. Office of Naval Research. D. Bélanger acknowledges the financial support of the Natural Science and Engineering Research Council of Canada. The Ministère Français des Affaires Etrangères of France and the Ministère des Relations Internationales of Québec are also greatly acknowledged for supporting this work. Part of the work contributed by O. Crosnier and T. Brousse was performed under the framework of the ABHYS French ANR project, whose support is also acknowledged. The authors gratefully acknowledge John R. Miller (JME, Inc.) for helpful discussions regarding the technical content of this article.

References

1. B.E. Conway, *Electrochemical Supercapacitors: Scientific Fundamentals and Technological Applications* (Kluwer Academic/Plenum Publishers, New York 1999).
2. B.E. Conway, *J. Electrochem. Soc.* **138**, 1539 (1991).
3. A. Burke, *J. Power Sources* **91**, 37 (2000).
4. R.A. Huggins, *Solid State Ionics* **134**, 179 (2000).
5. M. Conte, *Fuel Cells* **10**, 806 (2010).
6. A. Burke, *Int. J. Energy Res.* **34**, 133 (2010).
7. R.A. Rightmire, U.S. Patent 3,288,641 (November 29, 1966).
8. www.maxwell.com.
9. www.nesscap.com.
10. www.tecategroup.com.
11. E. Frackowiak, F. Béguin, *Carbon* **39**, 937 (2001).
12. E. Frackowiak, *Phys. Chem. Chem. Phys.* **9**, 1774 (2007).
13. L.L. Zhang, X.S. Zhao, *Chem. Soc. Rev.* **38**, 2520 (2009).
14. P. Simon, A. Burke, *ECS Interface* **17** (1), 38 (2008).
15. J. Biener, M. Stadermann, M. Suss, M.A. Worsley, M.M. Biener, K.A. Rose, T.F. Baumann, *Energy Environ. Sci.* **4**, 656 (2011).
16. H. Zhang, G.P. Cao, Y.S. Yang, *Energy Environ. Sci.* **2**, 932 (2009).
17. J. Chmiola, G. Yushin, Y. Gogotsi, C. Portet, P. Simon, P.L. Taberna, *Science* **313**, 1760 (2006).
18. M.D. Stoller, S. Park, Y. Zhu, J. An, R.S. Ruoff, *Nano Lett.* **8**, 3498 (2008).
19. J. Miller, R.A. Outlaw, B.C. Holloway, *Science* **329**, 1637 (2010).
20. N.A. Choudhury, S. Sampath, A.K. Shukla, *Energy Environ. Sci.* **2**, 55 (2009).
21. B.E. Conway, V. Birss, J. Wojtowicz, *J. Power Sources* **66**, 1 (1997).
22. P. Simon, Y. Gogotsi, *Nat. Mater.* **7**, 845 (2008).
23. X. Zhao, B.M. Sánchez, P.J. Dobson, P.S. Grant, *Nanoscale* **3**, 839 (2011).
24. T.C. Liu, W.G. Pell, B.E. Conway, S.L. Roberson, *J. Electrochem. Soc.* **145**, 1882 (1998).
25. D. Choi, G.E. Blomgren, P.N. Kumta, *Adv. Mater.* **18**, 1178 (2006).
26. G.A. Snook, P. Kao, A.S. Best, *J. Power Sources* **196**, 1 (2011).
27. J.P. Zheng, P.J. Cyang, T.R. Jow, *J. Electrochem. Soc.* **142**, 2699 (1995).
28. W. Dmowski, T. Egami, K.E. Swider-Lyons, C.T. Love, D.R. Rolison, *J. Phys. Chem. B* **106**, 12677 (2002).
29. R. Fu, Z. Ma, J.P. Zheng, *J. Phys. Chem. B* **106**, 3592 (2002).
30. W. Sugimoto, H. Iwata, K. Yokoshima, Y. Murakami, Y. Takasu, *J. Phys. Chem. B* **109**, 7330 (2005).
31. W. Sugimoto, H. Iwata, Y. Yasunaga, Y. Murakami, Y. Takasu, *Angew. Chem. Int. Ed.* **42**, 4092 (2003).
32. K. Fukuda, T. Saida, J. Sato, M. Yonezawa, Y. Takasu, W. Sugimoto, *Inorg. Chem.* **49**, 4391 (2010).
33. K. Fukuda, H. Kato, W. Sugimoto, Y. Takasu, *J. Solid State Chem.* **182**, 2997 (2009).
34. H. Kim, B.N. Popov, *J. Power Sources* **104**, 52 (2002).
35. M. Min, K. Machida, J.H. Jang, K. Naoi, *J. Electrochem. Soc.* **153**, A334 (2006).
36. K. Naoi, S. Ishimoto, N. Ogihara, Y. Nakagawa, S. Hatta, *J. Electrochem. Soc.* **156** A52 (2009).
37. C.N. Chervin, A.M. Lubers, J.W. Long, D.R. Rolison, *J. Electroanal. Chem.* **644**, 155 (2010).
38. C.B. Arnold, R.C. Wartena, K.E. Swider-Lyons, A. Piqué, *J. Electrochem. Soc.* **150**, A571 (2003).
39. W. Sugimoto, K. Yokoshima, K. Ohuchi, Y. Murakami, Y. Takasu, *J. Electrochem. Soc.* **153**, A255 (2006).
40. H.Y. Lee, J.B. Goodenough, *J. Solid State Chem.* **144**, 220 (1999).
41. D. Bélanger, T. Brousse, J.W. Long, *ECS Interface* **17** (1), 49 (2008).
42. Z.W. Zhang, G.Z. Chen, *Energy Mater.* **3**, 186 (2008).
43. W.F. Wei, X.W. Cui, W.X. Chen, D.G. Ivey, *Chem. Soc. Rev.* **40**, 1697 (2011).
44. M. Toupin, T. Brousse, D. Bélanger, *Chem. Mater.* **16**, 3184 (2004).
45. S.-L. Kuo, N.-L. Wu, *J. Electrochem. Soc.* **153**, A1317 (2006).
46. H. Kanoh, W. Tang, Y. Makita, K. Ooi, *Langmuir* **13**, 6845 (1997).
47. O. Ghodbane, J.-L. Pascal, F. Favier, *ACS Appl. Mater. Interfaces* **1**, 1130 (2009).
48. S.-C. Pang, M.A. Anderson, T.W. Chapman, *J. Electrochem. Soc.* **147**, 444 (2000).

49. T. Brousse, M. Toupin, R. Dugas, L. Athouël, O. Crosnier, D. Bélanger, *J. Electrochem. Soc.* **153**, A2171 (2006).
50. H.Y. Lee, S.Y. Kim, H.Y. Lee, *Electrochem. Solid-State Lett.* **4**, A19 (2001).
51. X. Dong, W. Shen, J. Gu, L. Xiong, Y. Zhu, H. Li, J. Shi, *J. Phys. Chem. B* **110**, 6015 (2006).
52. V. Subramanian, H.W. Zhu, B.Q. Wei, *Electrochem. Commun.* **8**, 827 (2006).
53. S.B. Ma, K.W. Nam, W.S. Yoon, X.Q. Yang, K.Y. Ahn, K.H. Oh, K.B. Kim, *J. Power Sources* **178**, 43 (2008).
54. T. Bordjiba, D. Bélanger, *J. Electrochem. Soc.* **156**, A378 (2009).
55. S. Zhang, C. Peng, K.C. Ng, G.Z. Chen, *Electrochim. Acta* **55**, 7447 (2010).
56. A.E. Fischer, K.A. Pettigrew, D.R. Rolison, R.M. Stroud, J.W. Long, *Nano Lett.* **7**, 281 (2007).
57. J. Yan, Z.J. Fan, T. Wei, W.Z. Qian, M.L. Zhang, F. Wei, *Carbon* **48**, 3825 (2010).
58. Y.C. Hsieh, K.T. Lee, Y.P. Lin, N.L. Wu, S.W. Donne, *J. Power Sources* **177**, 660 (2008).
59. F. Ataherian, K.-T. Lee, N.-L. Wu, *Electrochim. Acta* **55**, 7429 (2010).
60. T. Cottineau, M. Toupin, T. Delahaye, T. Brousse, D. Bélanger, *Appl. Phys. A* **82**, 599 (2006).
61. E. Raymundo-Pinero, V. Khomenko, E. Frackowiak, F. Béguin, *J. Electrochem. Soc.* **152**, A229 (2005).
62. S. Razoumov, S. Litvinenko, A. Beliakov, "Asymmetric electrochemical capacitor and method of making," U.S. Patent 6,222,723 (April 2001).
63. W.G. Pell, B.E. Conway, *J. Power Sources* **136**, 334 (2004).
64. www.esma-cap.com/@lang=English.
65. www.axionpower.com, see technology section (PbC® technology).
66. M.S. Hong, S.H. Lee, S.W. Kim, *Electrochem. Solid-State Lett.* **5**, A227 (2002).
67. T. Brousse, M. Toupin, D. Bélanger, *J. Electrochem. Soc.* **151**, A614 (2004).
68. V. Khomenko, E. Raymundo-Piñero, E. Frackowiak, F. Béguin, *Appl. Phys. A* **82**, 567 (2006).
69. F. Béguin, K. Kierzek, M. Friebe, A. Jankowska, J. Machnikowski, K. Juewicz, E. Frackowiak, *Electrochim. Acta* **51**, 2161 (2006).
70. X. Qin, X.P. Gao, H. Liu, H.T. Yuan, D.Y. Yan, W.L. Gong, D.Y. Song, *Electrochem. Solid-State Lett.* **3**, 532 (2000).
71. C. Vix-Guterl, E. Frackowiak, K. Jurewicz, M. Friebe, J. Parmentier, F. Béguin, *Carbon* **43**, 1293 (2005).
72. K. Jurewicz, E. Frackowiak, F. Béguin, *Appl. Phys. A* **78**, 981 (2004).
73. F. Béguin, M. Friebe, K. Jurewicz, C. Vix-Guterl, J. Dentzer, E. Frackowiak, *Carbon* **44**, 2392 (2006).
74. D. Qu, *J. Power Sources* **179**, 310 (2008).
75. M.J. Bleda-Martínez, J.M. Pérez, A. Linares-Solano, E. Morallón, D. Cazorla-Amorós, *Carbon* **46**, 1053 (2008).
76. K. Kalinathan, D.P. DesRoches, X.R. Liu, P.G. Pickup, *J. Power Sources* **181**, 182 (2008).
77. G. Pognon, T. Brousse, L. Demarconnay, D. Bélanger, *J. Power Sources* **196**, 4117 (2011).
78. H.A. Andreas, B.E. Conway, *Electrochim. Acta* **51**, 6510 (2006).
79. T. Brousse, D. Bélanger, *Electrochem. Solid-State Lett.* **6**, A244 (2003).
80. W.-H. Jin, G.T. Cao, J.Y. Sun, *J. Power Sources* **175** 686 (2008).
81. M.B. Sassin, A.N. Mansour, K.A. Pettigrew, D.R. Rolison, J.W. Long, *ACS Nano* **4**, 4505 (2010).
82. J. Santos-Peña, O. Crosnier, T. Brousse, *Electrochim. Acta* **55**, 7511 (2010).
83. K.C. Ng, S. Zhang, C. Peng, G.Z. Chen, *J. Electrochem. Soc.* **156**, A846 (2009).
84. K.H. Reiman, K.M. Brace, T.J. Gordon-Smith, I. Nandhakumar, G.S. Attard, J.R. Owen, *Electrochem. Comm.* **8**, 517 (2006).
85. L. Lu, Y. Zhu, F. Li, W. Zhuang, K.Y. Chan, X. Lu, *J. Mater. Chem.* **20**, 7645 (2010).
86. J.-Y. Luo, Y.-Y. Xia, *J. Power Sources* **186**, 224 (2009).
87. S. Sarangapani, in *Handbook of Solid State Batteries and Capacitors*, M.Z.A. Munshi, Ed. (World Scientific, Singapore, 1995), pp. 601.
88. M.D. Stoller, R.S. Ruoff, *Energy Environ. Sci.* **3**, 1294 (2010).
89. A. Burke, M. Miller, *Electrochim. Acta* **55**, 7538 (2010).
90. C. Peng, S. Zhang, X. Zhou, G.Z. Chen, *Energy Environ. Sci.* **3**, 1499 (2010).
91. L. Demarconnay, E. Raymundo-Piñero, F. Béguin, *J. Power Sources* **196**, 580 (2011).
92. A. Burke, M. Miller, *J. Power Sources* **196**, 514 (2011).
93. J.P. Zheng, *J. Electrochem. Soc.* **150**, A484 (2003).
94. *Battery Test Manual for Plug-in Hybrid Electric Vehicles*, U.S. Department of Energy, Vehicle Technology Program, INL/EXT-07–12536 (March 2008).
95. P.L. Taberna, P. Simon, J.F. Fauvarque, *J. Electrochem. Soc.* **150**, A292 (2003).
96. T. Brousse, P.L. Taberna, O. Crosnier, R. Dugas, P. Guillemet, Y. Scudeller, Y. Zhou, F. Favier, D. Bélanger, P. Simon, *J. Power Sources* **173**, 633 (2007).
97. Z.-S. Wu, W. Ren, D.-W. Wang, F. Li, B. Liu, H.-M. Cheng, *ACS Nano* **4**, 5835 (2010).
98. Y.-P. Lin, N.-L. Wu, *J. Power Sources* **196**, 851 (2011).
99. A. Yuan, X. Wang, Y. Wang, J. Hu, *Energy Convers. Manage.* **51**, 2588 (2010).
100. V. Khomenko, E. Raymundo-Piñero, F. Béguin, *J. Power Sources* **153**, 183 (2006).
101. Y.-G. Wang, Y.-Y. Xia, *J. Electrochem. Soc.* **153**, A450 (2006).
102. Q. Qu, L. Li, S. Tian, W. Guo, Y. Wu, R. Holze, *J. Power Sources* **195**, 2789 (2010).
103. A. Malak, K. Fic, G. Lota, C. Vix-Guterl, E. Frackowiak, *J. Solid State Electrochem.* **14**, 811 (2010).
104. P. Staiti, F. Lufrano, *Electrochim. Acta* **55**, 7436 (2010).
105. Z. Algharaibeh, P.G. Pickup, *Electrochem. Commun.* **13**, 147 (2011).
106. Z. Algharaibeh, X. Liu, P.G. Pickup, *J. Power Sources* **187**, 640 (2009).
107. V. Khomenko, E. Raymundo-Pinero, F. Béguin, *J. Power Sources* **195**, 4234 (2010).
108. N. Yu, L. Gao, *Electrochem. Commun.* **11**, 220 (2009).
109. G.M. Suppes, C.G. Cameron, M.S. Freund, *J. Electrochem. Soc.* **157**, A1030 (2010).
110. J.-W. Lang, L.-B. Kong, M. Liu, Y.-C. Luo, L. Kang, *J. Electrochem. Soc.* **157**, A1341 (2010).
111. H. Inoue, Y. Namba, E. Higuchi, *J. Power Sources* **195**, 6239 (2010).
112. K.-H. Chang, C.-C. Hu, C.-M. Huang, Y.-L. Liu, C.-I Chang, *J. Power Sources* **196**, 2387 (2011).
113. T. Brousse, D. Bélanger, *Electrochem. Solid-State Lett.* **6**, A244 (2003).
114. Y.-P. Lin, N.-L. Wu, *J. Power Sources* **196**, 851 (2011).
115. P. Guillemet, Y. Scudeller, T. Brousse, *J. Power Sources* **157**, 630 (2006).
116. A.D. Klementov, S.V. Litvinenko, A.V. Stepanov, I.N. Varakin, *Proceedings of the 11th Seminar on Double-Layer Capacitors*, Deerfield Beach, FL, USA, 3–5 December 2001.
117. H.A. Mosqueda, O. Crosnier, L. Athouël, Y. Dandeville, Y. Scudeller, P.H. Guillemet, D.M. Schleich, T. Brousse, *Electrochim. Acta* **55**, 7479 (2010).
118. T. Brousse, P.L. Taberna, O. Crosnier, R. Dugas, P. Guillemet, Y. Scudeller, Y. Zhou, F. Favier, D. Bélanger, P. Simon, *J. Power Sources* **173**, 633 (2007). □